

ANALYSIS OF LARGE SCALE NORMAL MODES

BY THE ECMWF ANALYSIS SCHEME

G.J. Cats and W. Wergen

ECMWF

Reading, U.K.

Abstract

The capability of the ECMWF optimum interpolation scheme to analyse large scale normal modes has been investigated in two series of experiments. The first used an idealised data coverage with one simulated sounding every 7.5° which reports height and wind at 15 pressure levels. The second series was based on an operational type data coverage. With the idealised data coverage the main error source is shown to be vertical and horizontal aliasing. In particular, the scheme is not able to distinguish between large scale Kelvin modes and large scale Rossby modes. Some of the reasons for the aliasing are discussed.

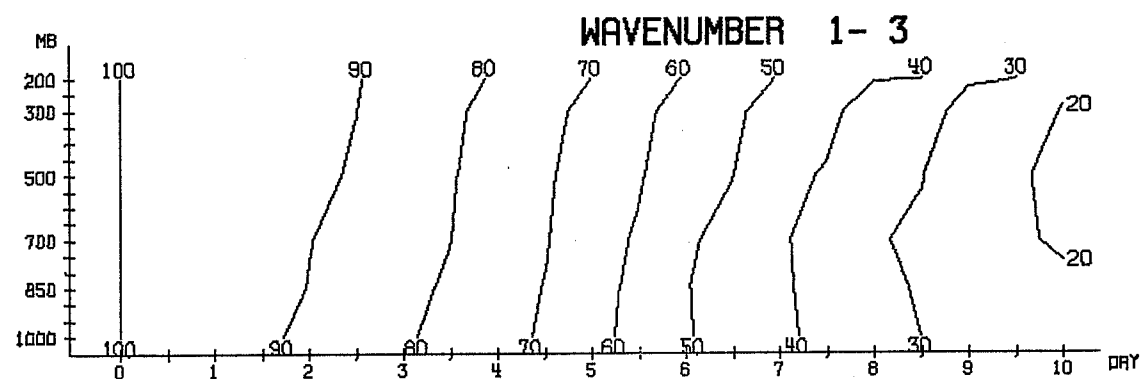
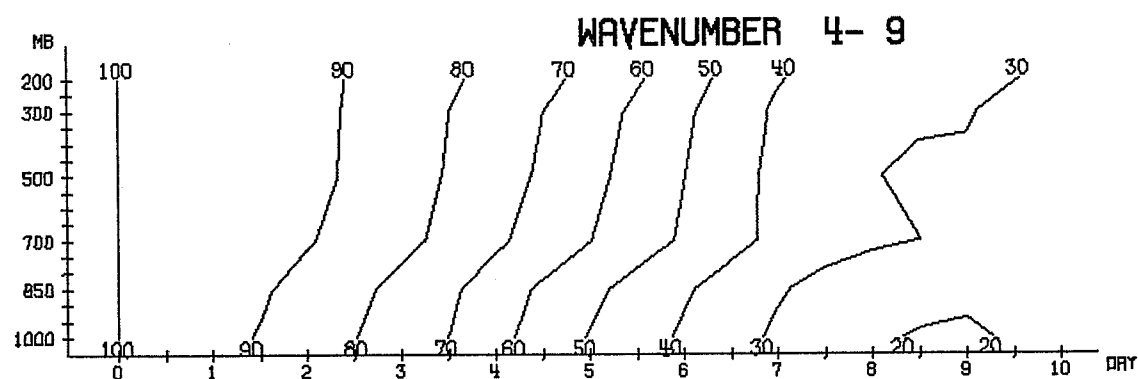
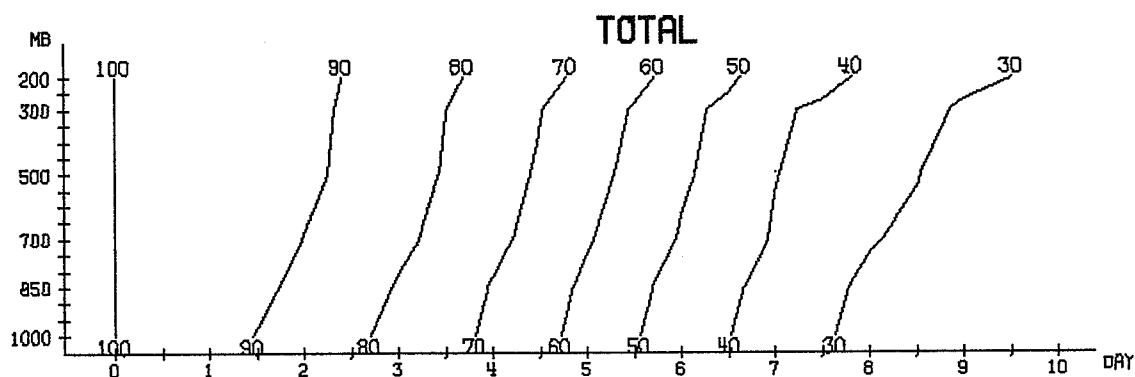
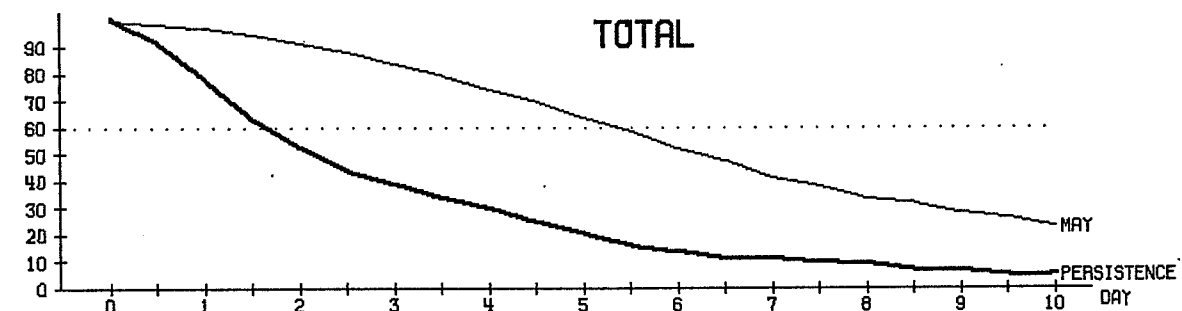
For an operational type data coverage, the analysis error increases considerably due to a poor analysis of the input mode. The prime reason for this is the irregular observation network, which -due to the local character of the optimum interpolation (O/I) scheme - inhibits the correction of large scale first-guess errors in data sparse regions. When aliasing on other modes is taken into account, the normalised RMS analysis error for some large scale modes can amount to 75%. Finally, the relative importance of tropical mass and wind observations for analysing some large scale modes is discussed.

1. INTRODUCTION

One of the problems in medium range weather prediction is the large discrepancy between the theoretical expectations and the operational achievements in forecasting the planetary scale waves. Fig. 1, which is taken from one of the quarterly forecast reports of the European Centre For Medium Range Weather Forecasts (ECMWF), shows that there is little difference in forecast skill between the planetary scale (wavenumbers 1 - 3) and the synoptic scale (wavenumbers 4 - 9). According to classical predictability theory, one should, however, expect a higher skill in predicting the long waves.

The present study tries to shed some light into this problem by investigating how well present day analysis systems analyse the large scale flow. We shall examine the performance of the global, three-dimensional, multivariate optimum interpolation scheme (Lorenc, 1981) in analysing model normal modes. These normal modes are the free solutions of the linearised model equations. They are global, three-dimensional structures, which combine the mass-and windfield. In other words they are just the structures the ECMWF O/I scheme is designed to analyse. Furthermore, they are meteorologically relevant structures, which have frequently been identified in observations (Venne and Stanford, 1982).

There are several reasons why a correct initial value for the long waves might be important. Firstly, many of these modes travel as free waves in forecast models (Wergen, 1983). Therefore, their time evolution is entirely dominated by their initial amplitude. Secondly, in the case of forcing, the forcing itself depends on the flow. For instance, convection might react



31 CASES MEAN BETWEEN 20.0 AND 82.5 N
ANOM-CORRELATION OF HEIGHT % MAY

Fig. 1 Averaged anomaly correlation of height (%) in the domain 20°N-82.5°N and 1000-200 mb. Top diagram : time evolution of total averaged scores for persistence and model forecasts. Other diagrams : time/pressure cross-sections of the model score calculated over various Fourier spectral bands (total, 4-9, 1-3). May 1982.

differently for a slow westward moving, dispersive Rossby wave than for a faster, highly divergent, non-dispersive, eastward moving Kelvin mode. Furthermore, initial errors in the planetary scale will interact non-linearly with smaller scales.

2. THE ANALYSIS SYSTEM

The ECMWF analysis scheme is one step in an intermittent data assimilation process, consisting of analysis, initialisation, and six-hour forecast. A full description can be found in Lorenc, 1981. Here, only the properties relevant for this study will be given.

Basically, the scheme acts as a linear operator which combines the irregularly spaced observations to yield values for mass, wind, and humidity at the regular model gridpoints. Only deviations from a first guess, interpolated to observation points, are analysed. The method used is a three-dimensional, multivariate extension of the "optimum interpolation" method. The required correlation functions are modelled as homogeneous and isentropic. Horizontally, a Gaussian function with a half width 'b' of 600 km is used (900 km in the southern hemisphere) for the height-height correlation. The height-streamfunction correlation is assumed to be 95% of its geostrophic value. In the tropics, this constraint is relaxed so that the scheme becomes univariate in height and wind at the equator. The vertical correlations, which are assumed to be separable from the horizontal ones, assume a hydrostatic relation between thicknesses and heights.

The global analysis domain is divided into 1196 sub-volumes (boxes), each having a side length of about 660 km. Within each volume, up to 191 individual pieces of information can be handled. If there are more data, various algorithms are used to reduce the number. However if there are less

than 191 observations, the search for data is extended to a distance of up to 2000 km from the centre of the box. A smoothing algorithm is used to ensure a smooth transition between neighbouring volumes. Within each box, the analysis scheme yields a non-divergent wind. Divergence can, therefore, only be analysed on scales larger than that of the box.

3. NORMAL MODES

The normal modes used in this study are the free solutions of the linearised, multi-level ECMWF gridpoint model. Although primarily used for initialisation purposes (Temperton and Williamson, 1981), they are also a powerful tool for diagnostic studies. Properly chosen, these modes are orthogonal and form a complete set. As the analysis scheme is a linear operator, it is possible to analyse each mode separately.

The vertical and horizontal structure of some selected normal modes is shown in Fig. 2. The first vertical mode (curve labelled 1 in Fig. 2a), also called the 'external mode', describes the barotropic part of the mass- and windfield. The second vertical mode, also called the first internal mode, changes sign near the tropopause. The third vertical mode changes sign near 400 mb and at around 50 mb; it is therefore important for describing processes which change sign in the troposphere, e.g. low level inflow and high level outflow of tropical convective systems. Generally, vertical mode k has $k-1$ zeros. With increasing order k the region of maximum amplitude moves towards the lower boundary.

Horizontally, the modes can be divided into two classes: the Rossby modes and the inertia-gravity modes. Within each class, they can be characterised by 3 indices: the superscript k for the vertical structure, and the subscripts m and n for the zonal wavenumber and the meridional index (e.g. a Rossby mode

is denoted by $R_{m,n}^k$). Fig. 2b shows half a wavelength of an external, zonal wavenumber $m=1$, gravest symmetric ($n=1$) Rossby mode (i.e. $R_{1,1}^1$). As the symmetry is known, it is sufficient to show only the northern hemisphere. In the extra-tropics the mass- and windfield are in approximate geostrophic balance. However in the tropics, where the geostrophic relation breaks down, normal modes still define a relation between mass- and windfield. For the same combination of horizontal indices m,n , modes with higher vertical index k are increasingly limited to the tropics (Figs. 2c and 2d). The gravest antisymmetric Rossby mode $R_{1,0}^1$ (Fig. 2e) is outstanding because its geostrophic character breaks down in middle latitudes. In the tropics, the flow is meridional with a large cross-isobaric component, which is more a feature of a gravity mode. This mode is also called the 'mixed Rossby-gravity mode'.

The gravest symmetric eastward gravity mode $E_{m,0}^k$ is also outstanding within the class of gravity waves; it has a very small meridional wind component and their zonal wind is in approximate geostrophic balance. These modes are also called 'Kelvin' modes (Figs. 2f and 2g). Finally, as is evident from Fig. 2h and Fig. 2i, the westward gravity modes W (and also the remaining eastward gravity modes) are highly divergent and ageostrophic. Because of its constraints (geostrophy and non-divergence) the analysis system can only be expected to work well when analysing Rossby modes, and to some extent Kelvin and mixed Rossby-gravity modes. Therefore, only these modes will be used in the following experiments.

4. DESIGN OF THE EXPERIMENTS

The basic idea of these experiments is to design a system in which the correct answer is already known everywhere in advance. To achieve this, the following strategy, sketched in Fig. 3, has been applied.

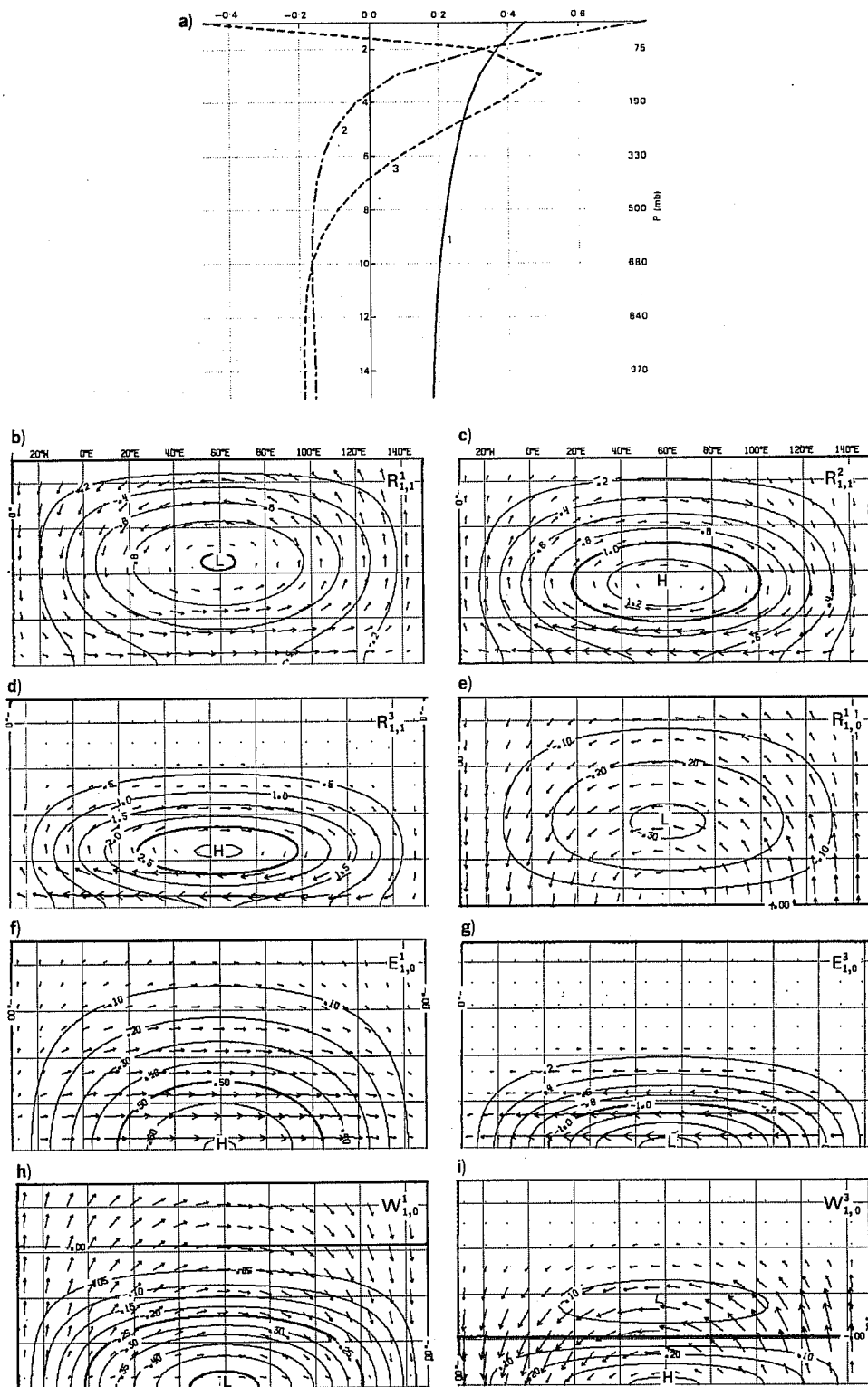


Fig. 2 Vertical (a) and horizontal structures (b-i) of modes used in the experiments. Panels show horizontal structures of temperature and wind field in Northern hemisphere for half a wave length. Grid distance is 20° .

- b - d Rossby modes
- e external, mixed Rossby gravity modes
- f, g Kelvin modes
- h, i westward inertia-gravity modes.

See text for notation.

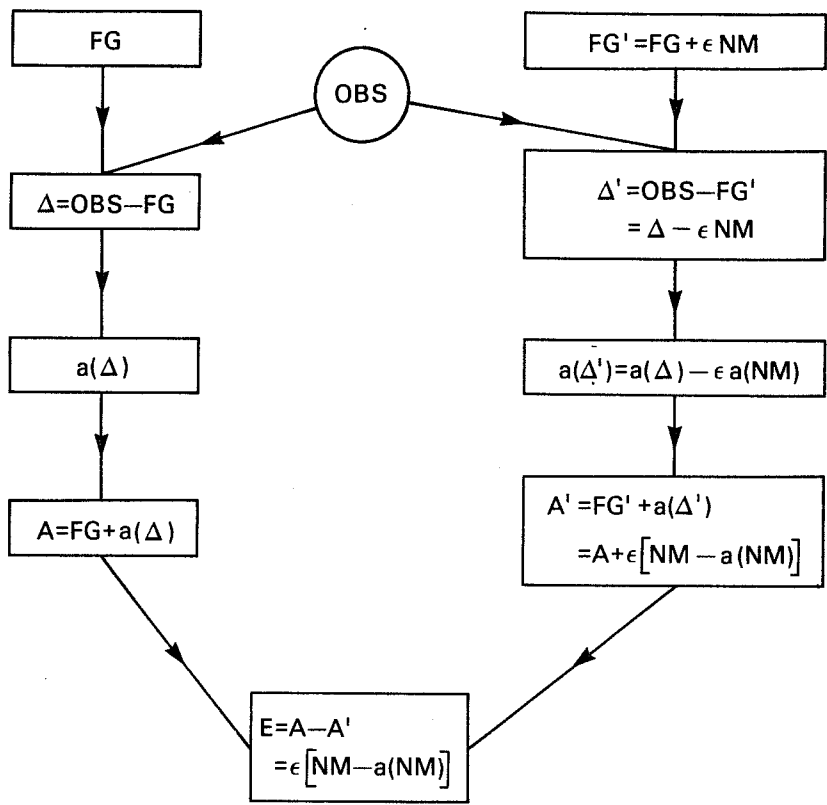


Fig. 3 Experimental set-up. See text for details.

First a normal analysis is performed (left hand branch in Fig. 3). This consists of the following steps:

- Take a first guess FG (which is a six hour forecast from the previous analysis)
- Collect the observations OBS
- Form the increment field $\Delta = \text{OBS} - \text{FG}$ at observation points
- Analyse the increment field; i.e. interpolate from the irregularly spaced observing points to the regular model grid
- Add the analysed increments $a(\Delta)$ to the first guess FG to yield the final analysis $A = \text{FG} + a(\Delta)$.

In the second scan (right hand side of Fig. 3), the above steps are repeated but with a modified first guess FG' . The modification is done by subtracting a multiple of a particular normal mode NM. In the perfect case, when the final analyses are entirely defined by the observations OBS, the analyses A and A' should be identical. However due to the way the statistical interpolation scheme is implemented, the first guess will be reflected in the final analyses A and A' according to the ratio of the assigned first guess and observation errors. As all operations involved are linear, the operations on sums are identical to the sums of the operations. Therefore, by computing the difference E between A and A', the original analyses A cancel and we are left with the analysis error for the normal mode NM only, which should be zero for a perfect system.

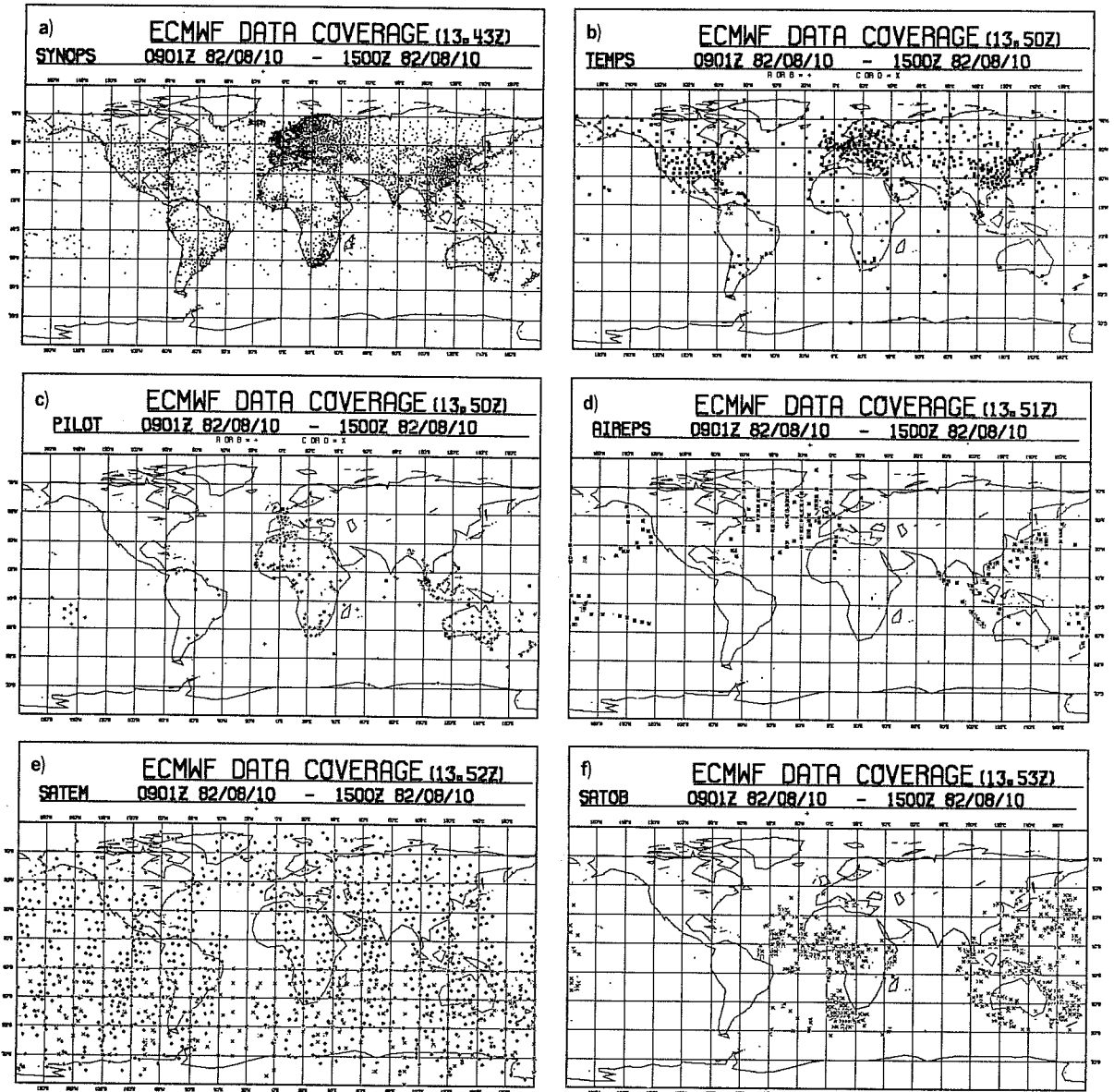


Fig. 4 Operational data coverage for 10.8.1982, 0901 GMT - 1500 GMT as received at ECMWF.

4.1 The idealised observation set

In order to study the systematic deficiencies of the ECMWF analysis scheme in analysing the large scale flow, it is necessary to exclude errors caused by the data distribution as much as possible. Therefore, we decided to construct an idealised observation set with one sounding every 7.5°. Poleward of 60° latitude the longitudinal spacing was increased to 15°. The observed values were derived from a model gridpoint file chosen at random (first guess for the operational analysis of 12 GMT, 22 November 1981). Data were derived for the 15 standard pressure levels between 1000 mb and 10 mb. The current radiosonde format was used: geopotential height accurate to 1 m, wind speed to 1 m/s, direction to 1°. The number of radiosondes manufactured was 960 yielding 43200 'observed' data. This is slightly more than the average number of data in a real data set. However, the idealised observations are regularly distributed and contain no errors. Therefore, the data checking part of the analysis scheme was not used. As the observations OBS are derived from the first guess FG, the increment Δ is zero, which makes the left hand branch of Fig. 3 redundant.

4.2 The real data set

For the experiments with a realistic data set, the data for 12GMT, 10 August 1982 were used. Fig. 4 shows the data coverage as received operationally at ECMWF. All observations valid from 0901 GMT to 1500 GMT are indicated. Note the poor data coverage in the tropics and in the southern hemispheric oceans. In particular, there are no wind observations in the tropical eastern Pacific. Furthermore, the ECMWF scheme uses mass observations from satellites (SATEM's) over land only above 100 mb and wind observations from satellites (SATOB's) only over sea.

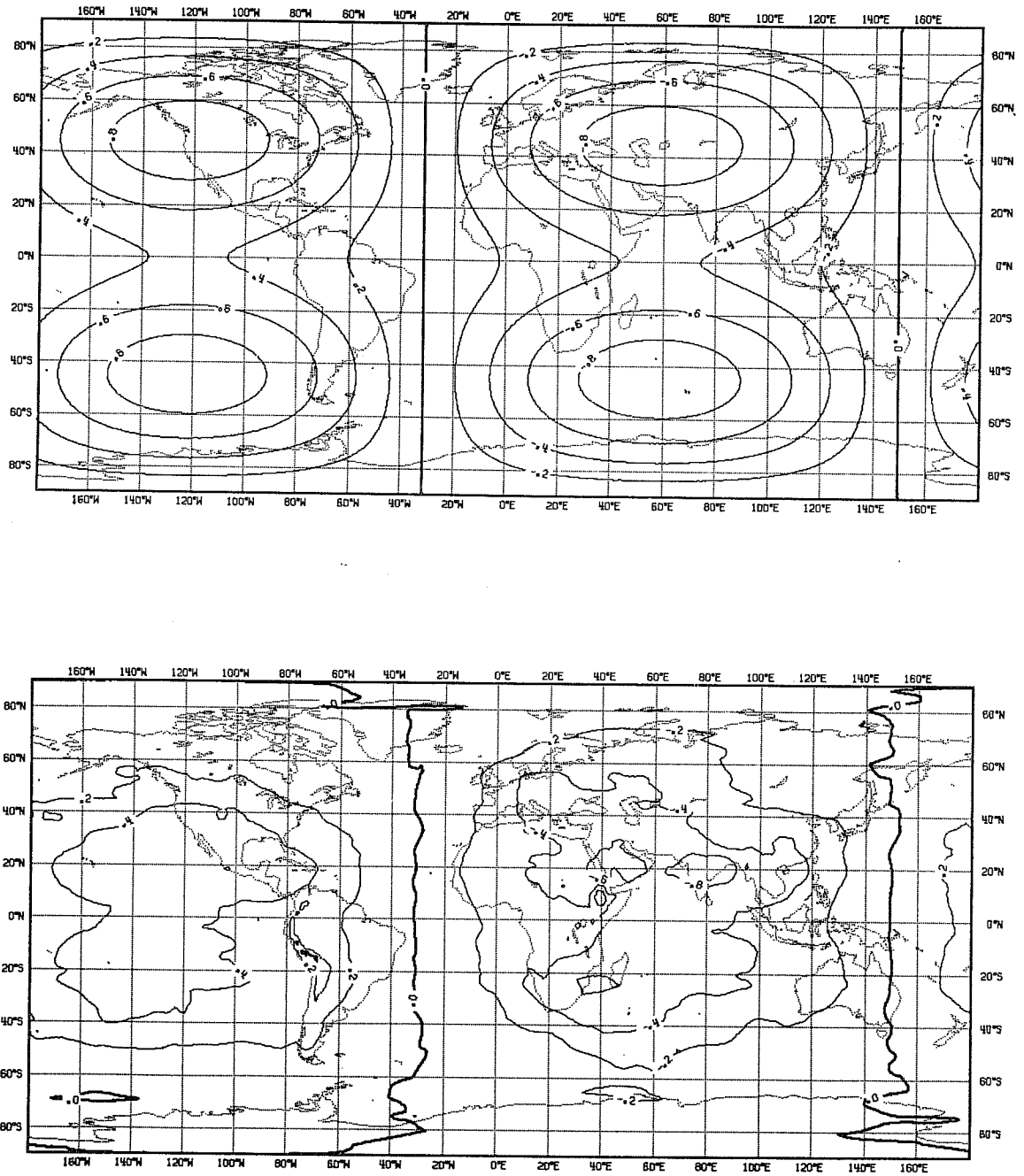


Fig. 5 Input temperature structure (top) at level 4 (≈ 200 mb) and analysis error (bottom) for external Rossby mode $R_{1,1}^1$ using idealised data coverage.

Operational data checking algorithms were included in the two analyses. Due to the differences in the first guesses, this led to a slightly different treatment for a small number of data in the two scans. We decided not to intervene because data checking is a vital ingredient of any analysis scheme and the imposed first guess differences (wind speed differences not greater than 2m/s) were considered to be realistic.

5. EXPERIMENTS USING THE IDEALISED DATA COVERAGE

5.1 Error structure

In the first experiment, the external, zonal wavenumber 1, gravest symmetric Rossby mode $R_{1,1}^1$ (5 day wave) was presented to the analysis system. Fig. 5(top) shows the input temperature structure (FG'-FG) at model level 4 (≈ 200 mb) whilst the analysis error (A'-A) at the same level is given in Fig. 5(bottom). Overall the analysis error is acceptable in the extra-tropics. However, it reaches the 100% level in the tropics. Note that the error is mainly in the amplitude.

As a normal mode consists of three-dimensional fields of mass and wind, it would be necessary to show the temperature and wind errors for all 15 levels in order to get a complete picture. Instead, the error field was projected back onto the normal modes. For the first 5 vertical modes the normalised RMS amplitude error was computed separately for Rossby modes, and westward and eastward gravity modes. Fig. 6a shows such an error spectrum for the $R_{1,1}^1$ mode. The vertical mode number is indicated on the abscissa; the curves are for the Rossby modes (dashed), the eastward gravity modes (dashed-dotted) and for the westward gravity modes (full). For a perfect system, all error amplitudes should be zero. In the O/I formulation the first guess gets some credit which results in a non-zero amplitude for the input mode. In all diagrams of this type, a dot will indicate the relative amplitude error for

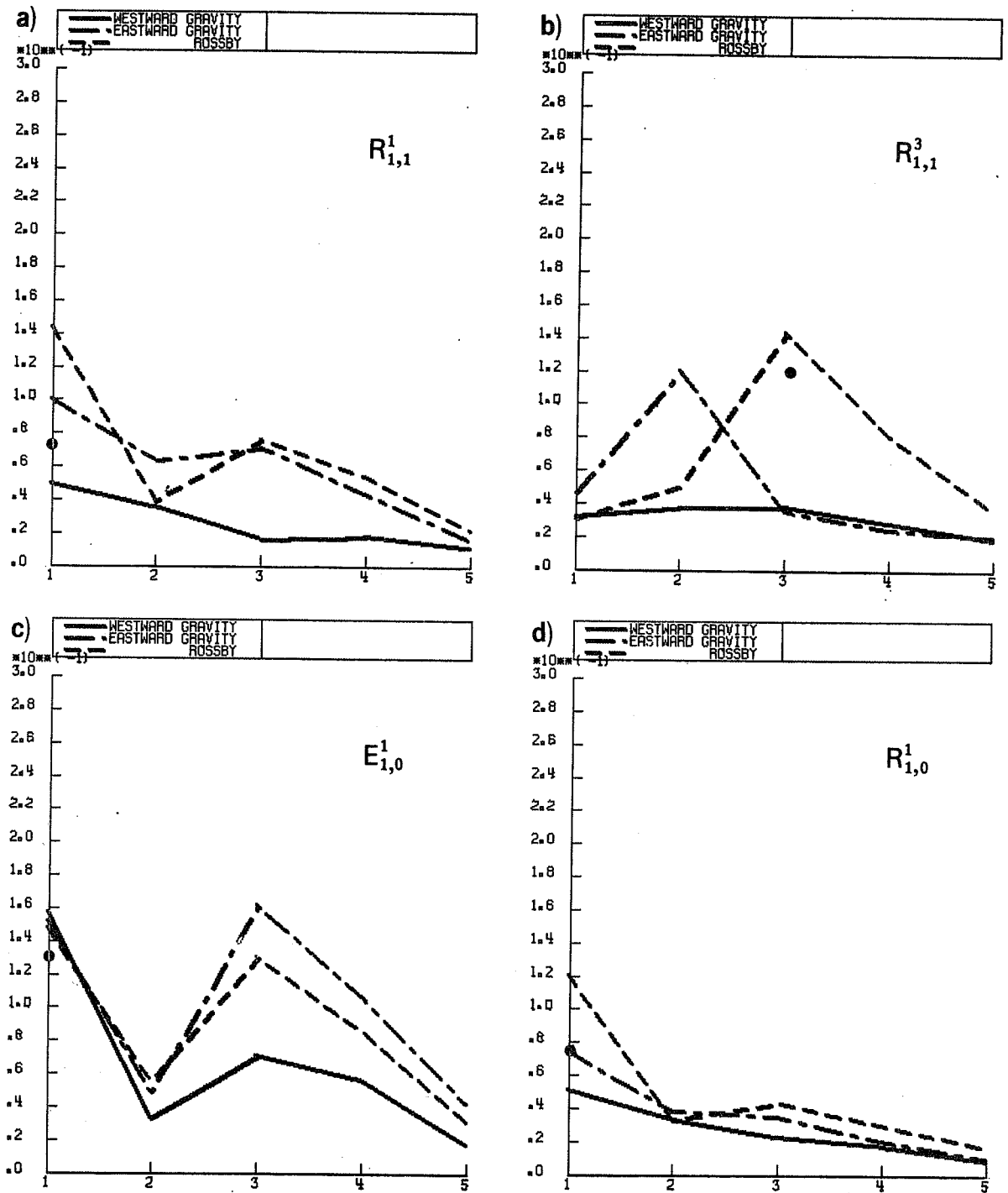


Fig. 6 Normalised RMS analysis errors as a function of vertical mode for idealised data coverage. Errors are given separately for Rossby (dashed), eastward gravity (dashed-dotted) and westward gravity (full). The dot on the ordinate gives the analysis error in the input mode only.

Panels show analysis error of :

- a) external Rossby mode $R_{1,1}^1$
- b) second internal Rossby modes $R_{1,1}^3$
- c) external Kelvin mode $E_{1,0}^1$
- d) external mixed Rossby-gravity mode.

the input mode itself. For the present example, this error amount to 8%, a result consistent with the assumed errors in the O/I formulation. However, an unwanted result is the excitation of other horizontal and vertical modes. Vertically, baroclinic structures not present in the input are generated by the scheme. Horizontal aliasing leads to the excitation of other Rossby modes (mainly with a higher meridional index) and of eastward moving gravity modes (mainly Kelvin). When aliasing is taken into account, the RMS analysis error for this case amounts to 23%. For the analysis of the second internal, gravest symmetric Rossby mode $R_{1,1}^3$, we get a similar result (Fig. 6b). The error in the input mode amounts to 12%. Horizontal aliasing is generally smaller than for the external Rossby mode. A severe problem is the aliasing on the first internal eastward gravity modes.

Fig. 6c shows the result for the external, zonal wavenumber 1 Kelvin mode $E_{1,0}^1$. The amplitude error in the input mode is 13%. Horizontally, Rossby and westward gravity modes are excited. Furthermore, severe aliasing on baroclinic Rossby and eastward gravity modes is evident. The overall analysis error for this mode is 38%. Since this mode only partially fulfills the requirements built into the analysis scheme, a poorer result than for the Rossby modes was to be expected.

Finally, we come to the external mixed Rossby-gravity mode $R_{1,0}^1$ (Fig. 5d). The amplitude error for the input mode is 7%. Again, other Rossby and eastward gravity modes are excited. Vertical aliasing is, however, small. When compared to the Kelvin mode (Fig. 6c), the analysis for the mixed Rossby-gravity mode is better. One of the reasons is that this mode is in approximate geostrophic balance in higher latitudes, which is not the case for the meridional component of the Kelvin mode.

5.2 Response matrix

While the error spectra contain most of the information, they do not reveal how the errors are distributed within the three classes of modes. Therefore, in Table 1 the errors are split up for individual modes with the same zonal wavenumber and the corresponding meridional index. Since the phase is hardly influenced, only the error in the real part of the complex error coefficient is given. The errors are normalised by the coefficient of the input mode and expressed as a percentage. Each row stands for a different input mode. The main diagonal element gives the analysis error in the input mode, the remaining entries show the aliasing onto other modes. Elements smaller than 6% are not shown. For a perfect system all elements should be zero.

Input \ Result	$R_{1,1}^1$	$R_{1,1}^2$	$R_{1,1}^3$	$E_{1,0}^1$	$E_{1,0}^2$	$E_{1,0}^3$
$R_{1,1}^1$	8		6	9		-7
$R_{1,1}^2$		16			14	8
$R_{1,1}^3$			12		-12	
$E_{1,0}^1$	10		13	13		-15
$E_{1,0}^2$		15	-10		21	12
$E_{1,0}^3$		10			7	16

Table 1. Response matrix of the analysis operator for the idealised data set. See text for details.

The matrix is not diagonally dominant, which shows that aliasing between Kelvin and Rossby modes is as important as the poor analysis of the input mode itself. One of the consequences of these results is that normal mode spectra obtained from the current O/I analysis scheme should be interpreted with some caution.

6. EXPERIMENTS WITH AN OPERATIONAL DATA COVERAGE

In this section we shall discuss the results from experiments using the operational data coverage from 12GMT, 10 August 1982. We shall present the results in the same form as in the previous chapter.

Fig. 7a gives the result for the $R_{1,1}^1$ mode. An alarming result is the 40% error level for the input mode (compared to 8% with the idealised data set). This suggests that present day observing systems lead to large errors in the planetary scale flow because current analysis systems do not correct large scale errors in data sparse areas. Aliasing on higher zonal and meridional indices leads to a 60% error in the external Rossby modes only. The vertical aliasing problem is still present although masked by the large horizontal errors. When summing over all amplitudes, the overall analysis error amounts to 75%.

The poor performance in analysing the planetary scales with a realistic network can also be seen for the $R_{1,1}^3$ mode (Fig. 7b). Again, the analysis error in the input mode is 40%. Strong aliasing on other horizontal and vertical modes also shows up. Note that the worst result is obtained for the external Kelvin mode $E_{1,0}^1$ (Fig. 7c); the input error is 55%, but a similar amount of error is caused by horizontal aliasing on other Rossby modes. The overall analysis error is close to 100%! As with the idealised data set, this is partially due to the geostrophic constraint imposed by the scheme in the extra-tropics, which does not hold for the meridional wind component of a Kelvin mode. This mode is however present in the atmosphere (Holton, 1979) and in atmospheric models (Hayashi and Gouder, 1978) and we should therefore try to analyse it more accurately. The analysis of the second internal

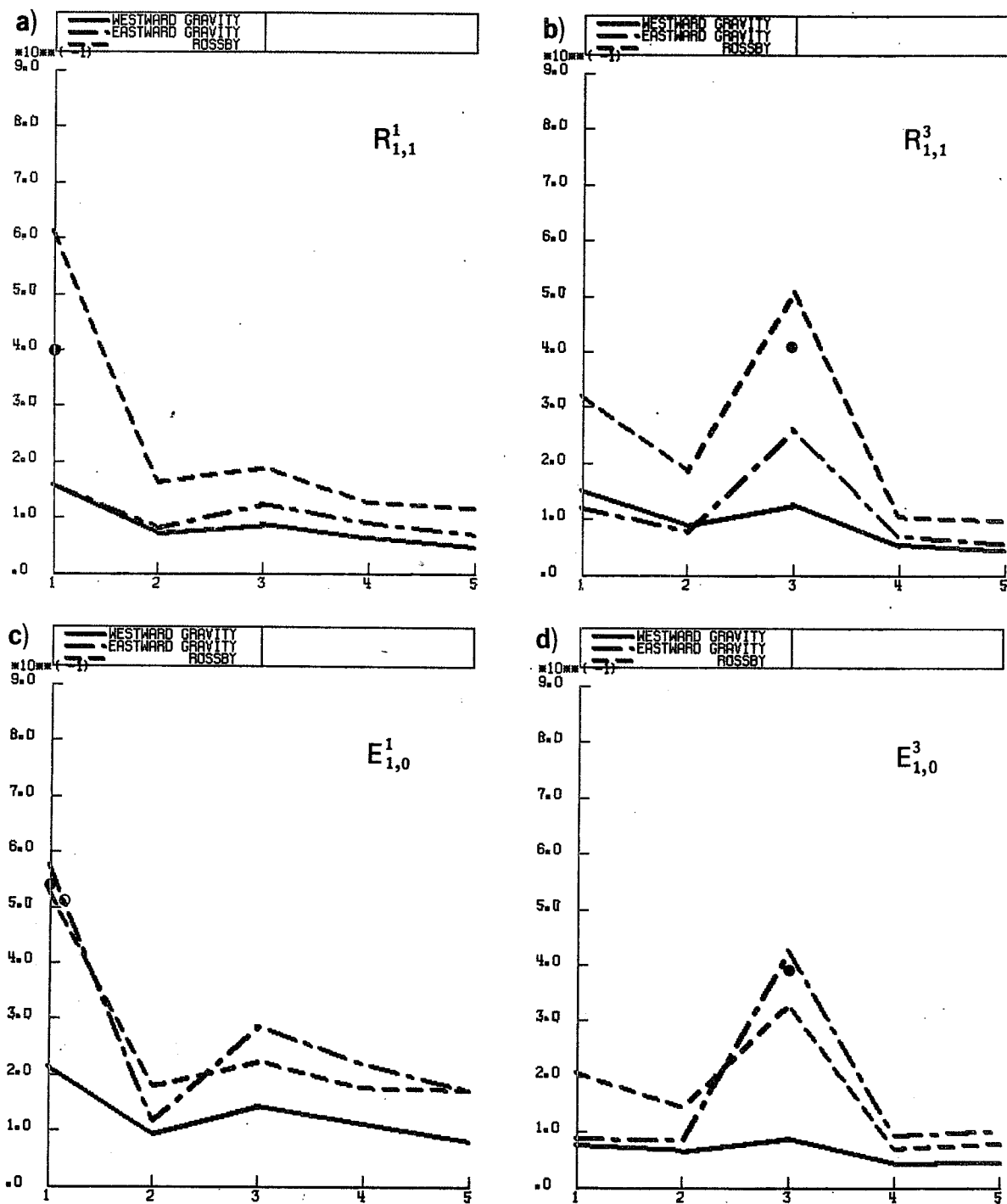


Fig. 7 Similar to Fig. 6, but for operational data coverage. Panels show analysis error of :
 a) external Rossby mode $R_{1,1}^1$
 b) second internal Rossby mode $R_{1,1}^3$
 c) external Kelvin mode $E_{1,0}^1$
 d) second internal Kelvin mode $E_{1,0}^3$

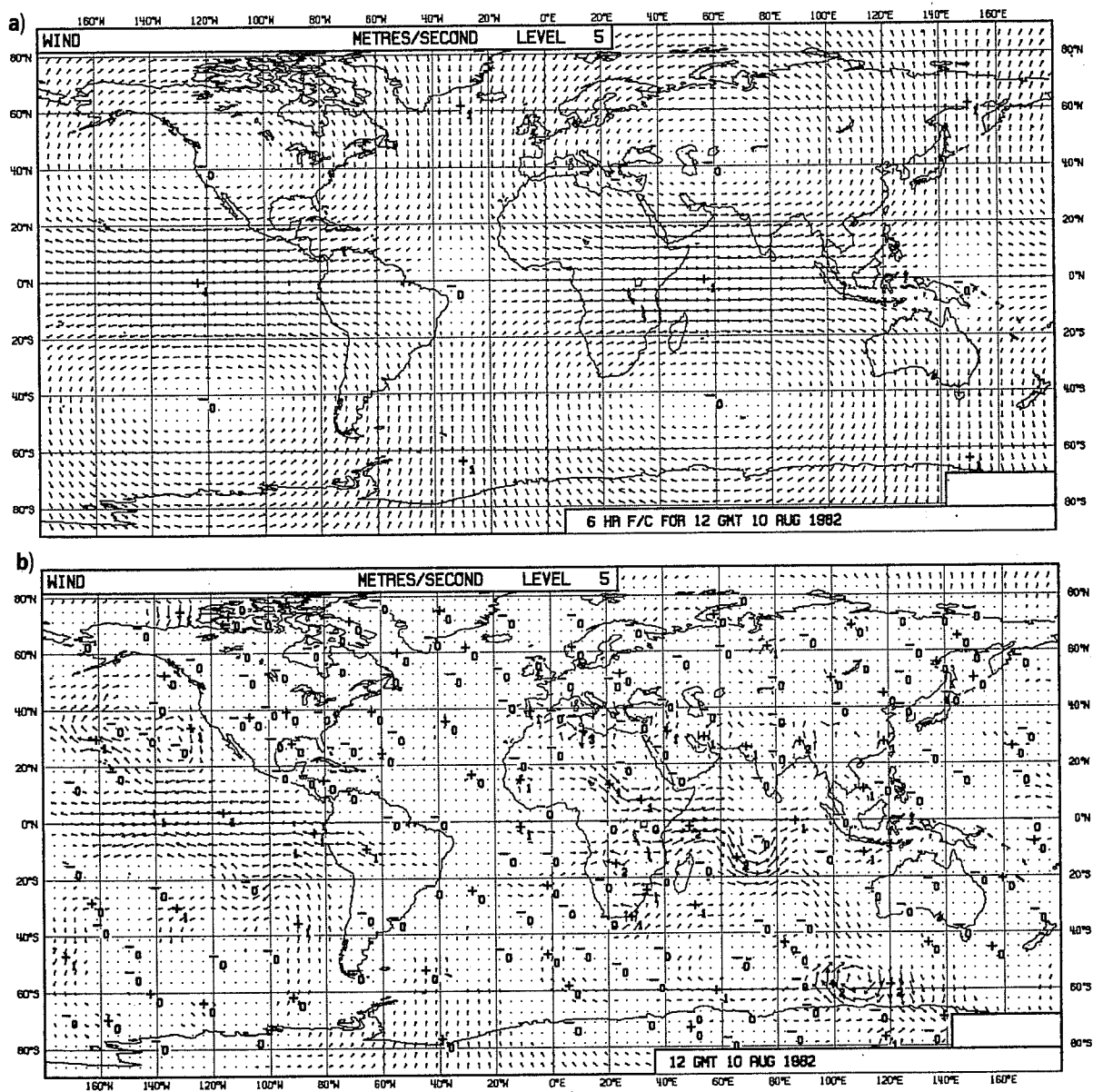


Fig. 8 Input wind field (top) at model level 5 (≈ 250 mb) and analysis error (bottom) when using operational data coverage. Numbers indicate wind speeds in m/sec.

Kelvin mode $E_{1,0}^3$ (Fig. 7d) is somewhat better. It is confined to the tropics, where the geostrophic constraint is relaxed in the ECMWF scheme. Therefore, aliasing on Rossby modes is smaller than for an external Kelvin mode. Nevertheless, the analysis errors are considerable.

In order to get an idea of the geographical distribution of the analysis errors, Fig. 8 shows the input (top) and the error (bottom) in the windfield at level 5 (≈ 250 mb) for the $R_{1,1}^1$ mode. In the tropics, this chart more or less reflects the availability of wind data. The winds in the tropical eastern Pacific are not analysed at all. To a lesser extent this is also true for the winds in the Indian ocean. Obviously, the winds will not be analysed as a wavenumber one pattern but will be aliased on smaller scales.

7. SENSITIVITY STUDIES

In section 5 it was shown that even with the idealised data coverage there are problems in analysing the large scale flow. In this section we shall try to shed some light into these results by studying the response to a variation of some external and internal parameters of the analysis scheme.

7.1 Vertical aliasing

One of the unwanted features of the ECMWF scheme is the change in the vertical structure. For example, when presented with a barotropic mode, the scheme introduces baroclinic structures.

In order to separate the horizontal aliasing problem from the vertical, the horizontal first-guess error correlations were eliminated. The analysis is therefore one-dimensional (in the vertical) and univariate in mass and wind. In Fig. 9 the vertical profiles for the input height field (light dashed), and for the analysis error at the equator (full) and at 45°S (dashed) are

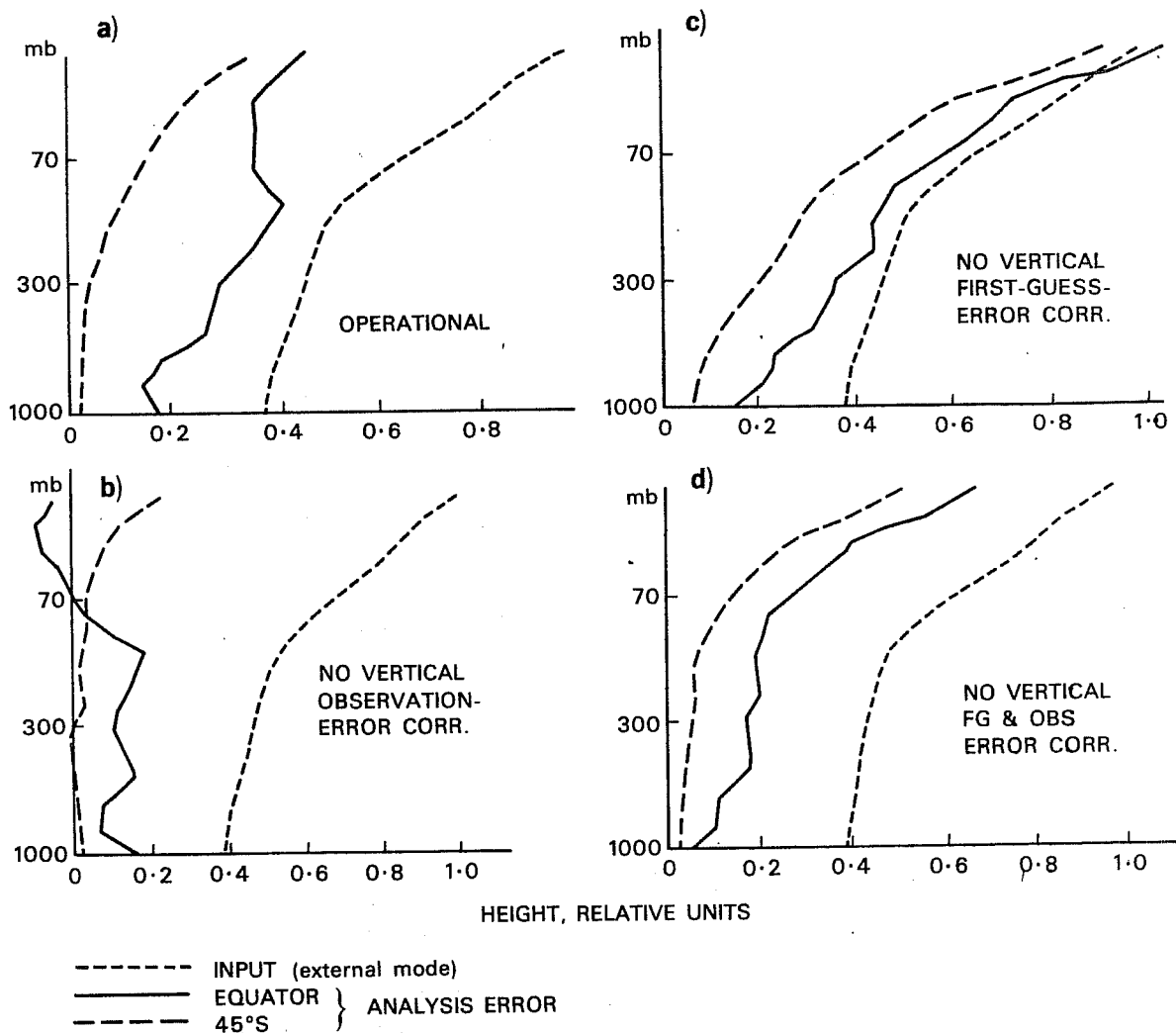


Fig. 9 Input height (light-dashed), corresponding to an external mode and analysis error at equator (full) and 45°S (dashed) for a one dimensional (vertical), univariate analysis scheme with observation at 15 levels. Analysis has been done at observation points. Panels show results for :

- a) operational formulation
- b) no vertical observation error correlation
- c) no vertical first guess error correlation
- d) no vertical correlation at all.

shown for different versions of the scheme. All profiles are taken at observation points; the values are normalised by the input height amplitude at 10 mb. Fig. 9a shows the result obtained using the operational version of the vertical first guess and observation error correlation. As in Fig. 5, the poor height analysis in the tropics stands out. However, when the vertical observation error correlation is switched off, the height analysis is improved (Fig 9b). There are some problems, though, in the tropics which can only be caused by the vertical first guess error correlation. Fig. 9c shows the result for the reverse configuration: no first guess error correlation but observation error correlation included. The analysis is indeed very poor in the upper levels. The last panel (Fig. 9d) shows the errors for the case when all vertical correlations are switched off. The result, which now simply reflects the different weights given to observations and first guess, can of course only be obtained for this type of data distribution with an observation at every analysis level.

These experiments show that there are serious problems in the vertical analysis of height, especially in the tropics. These results are consistent with the findings by Andersen (1983) who showed that the weights given in the vertical lead to serious problems in the height analysis. The present formulation of the vertical observation error correlation for height deteriorates the height analysis rather than improves it. In a multi-variate context this will also impact on the wind field. The poor height analysis will result in a poor analysis of those normal modes which have (like the Kelvin modes) a small ratio between kinetic energy and total energy.

7.2 Horizontal aliasing

Apart from vertical aliasing, there was considerable aliasing on other horizontal modes in the experiments using the idealised data coverage. Two

sets of experiments have been done in order to clarify the role of two components of the analysis scheme

- the local character

- the tropical mass-wind coupling

As described in Section 2, the analysis scheme is a local operator which tries to fit the observations within a particular scale only. This scale is defined by the half width 'b' of the Gaussian correlation function and by the radius for the data search, which is also related to 'b'. Operationally, 'b' is 600 km in the northern hemisphere and 900 km in the southern hemisphere with a transition zone in the tropics. This scale is probably not adequate for analysing structures with a wavelength of the order of 10^4 km. Therefore, the analysis of the $R_{1,1}^1$ mode was rerun with twice the standard value of 'b'. Fig. 10b shows the error spectrum for this experiment, which is to be compared with the standard experiment (Fig. 10a). The analysis error in the input mode remains unchanged. However, the aliasing on other Rossby modes is smaller. Also, the erroneous excitation of eastward gravity modes has become less severe. As a side effect, aliasing on other vertical modes has also become marginally smaller.

This result suggests that the large scale analysis can be improved by optimising the response of the analysis operator for the scales being analysed. In a realistic context, this would require a multi-pass system, where each pass is designed for a particular spectral band.

Another possible shortcoming of the multivariate ECMWF scheme is the mass-wind coupling in the tropics. As there is no locally applicable coupling,

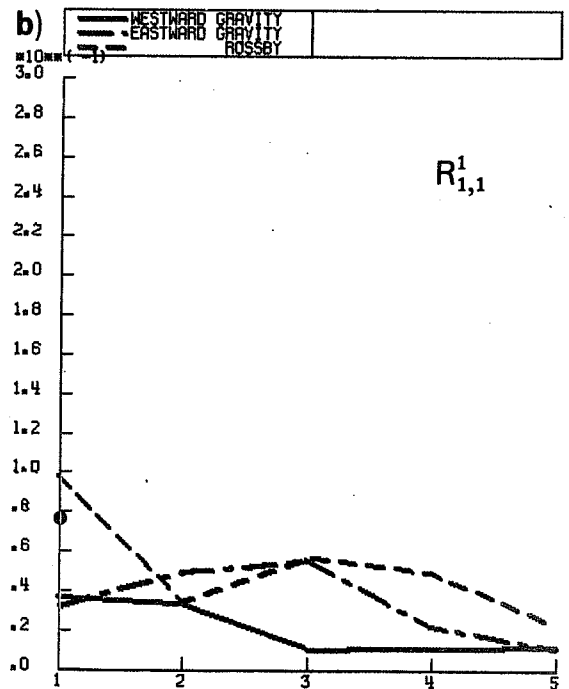
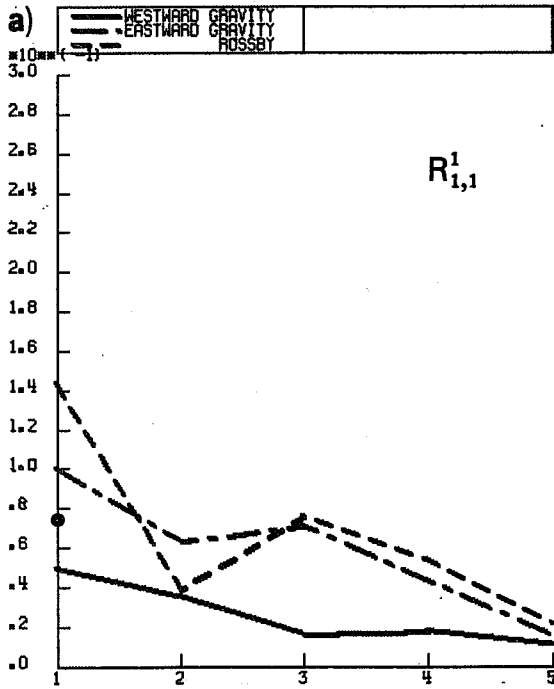


Fig. 10 Similar to Fig. 6, but analysis of external Rossby mode $R_{1,1}^1$ with operational scheme (a) and with twice the half width of the Gaussian correlation function (b)

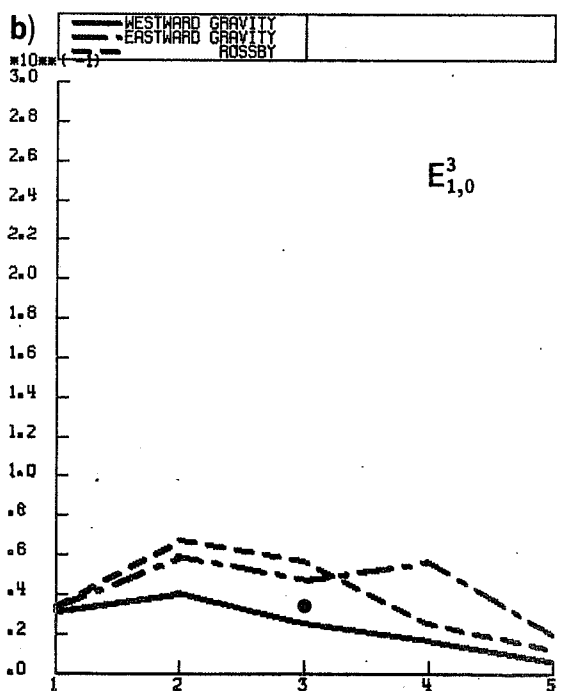
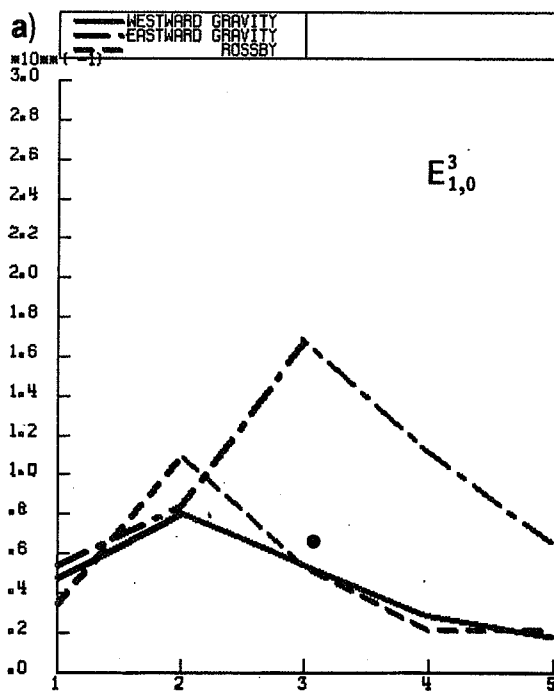


Fig. 11 Similar to Fig. 6, but analysis of second internal Kelvin mode $E_{1,0}^3$ with operational scheme (a) and reformulated tropical mass-wind relation (b).

the scheme gradually decouples the mass and wind analysis equatorward of 30° latitude. The actual formulation involves a manipulation of the Coriolis parameter f and yields a rather crude approximation for $\beta=df/dy$. It is, however possible to devise a more accurate algorithm. The details will not be given here, but the impact of this revision on the tropical analyses will be discussed. Fig. 11a shows the error spectrum for the second internal Kelvin mode $E_{1,0}^3$ as obtained from the current operational formulation of the scheme. Again, serious aliasing on other horizontal and vertical modes can be found. For the experiment with the reformulated mass-wind relation in the tropics (Fig. 11b), the analysis is much better; in particular the horizontal aliasing is less severe. Similar results apply also to other modes (not shown), although the impact is usually not as dramatic as for the above example.

7.3 Relative importance of tropical mass and wind observations

In the extra-tropics, the multivariate scheme is able to generate a wind analysis from height observations and vice versa. In the tropics the availability of both mass and wind observations is crucial for a good analysis. In this subsection we shall discuss how the lack of subsets of tropical data within the idealised data set influences the analysis.

We start with the external Rossby mode $R_{1,1}^1$. Fig. 12a shows the error spectrum for an analysis with all mass observations within 30° of the equator removed. Comparison of this figure with Fig. 6a shows that the horizontal analysis has deteriorated because of the lack of tropical mass data. In particular, the error in the external eastward gravity modes (mainly Kelvin) is as large as in the Rossby modes. Vertical aliasing is slightly smaller, which again indicates that the vertical aliasing is to a large extent caused by the poor tropical height analysis.

When analysing an internal Rossby mode $R_{1,1}^3$, the impact of tropical mass information is more pronounced (Fig. 12b). Compared to the results with the full data coverage (Fig. 6b), the horizontal analysis of Rossby and Kelvin modes is considerably worse (note the different scale in the ordinate of Fig. 12b). Without tropical mass data, the scheme has severe problems in separating Rossby modes from Kelvin modes. Note, that the error in the Rossby modes is dominated by the poor analysis of the input mode itself. Again, vertical aliasing is hardly influenced.

When analysing an internal Kelvin mode $E_{1,0}^3$ (Fig. 12c) without tropical mass data, the analysis errors get very large when compared to the full data coverage analysis (Fig. 11a). This again underlines the importance of tropical mass data for a proper separation between Rossby and Kelvin modes. As half of the total energy of a Kelvin mode is potential energy, (Longuet-Higgins, 1968), the importance of tropical mass data might have been anticipated.

Finally, to demonstrate the importance of tropical wind data, the $R_{1,1}^3$ mode has been analysed without tropical wind data (Fig. 12d). Compared to the no mass data case (Fig. 12 b), the analysis error in the input mode is twice as large when the wind information is missing. This shows the priority of wind data when analysing Rossby modes. Again, strong aliasing on Kelvin modes occurs.

Overall, the results of these experiments are in agreement with predictability theory, which stresses the importance of the tropical wind field. A worrying result, however, is the requirement for high-quality mass data in order to separate Rossby modes properly from Kelvin modes.

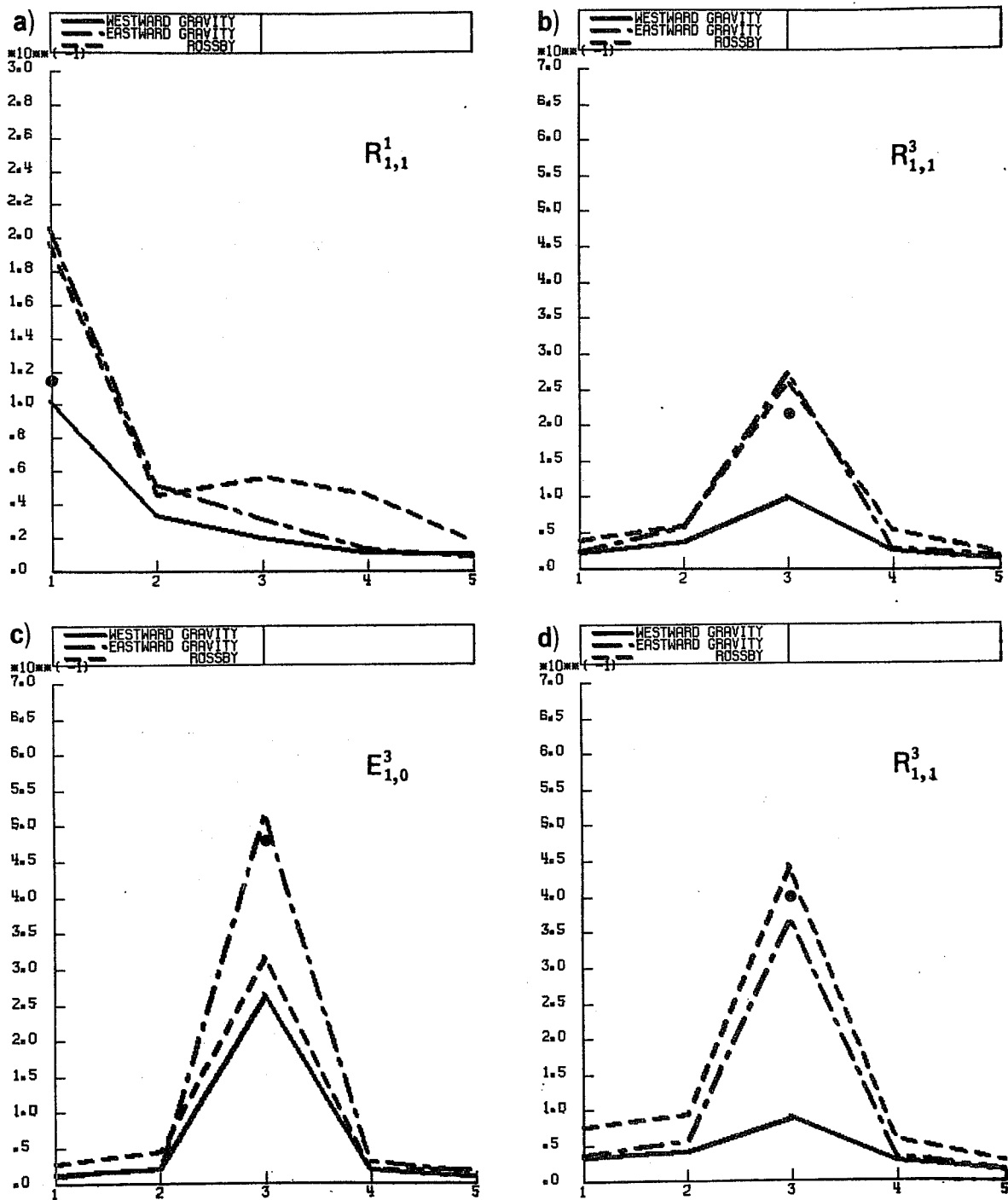


Fig. 12 Similar to Fig. 6, but with subset of the idealized data coverage
 Panels show the analysis errors for

- a) external Rossby $R_{1,1}^1$ without tropical mass data
- b) second internal Rossby mode $R_{1,1}^3$ without tropical mass data
- c) second internal Kelvin mode $E_{1,0}^3$ without tropical mass data
- d) second internal Rossby mode $R_{1,1}^3$ without tropical wind data

8. DISCUSSION

The performance of the global, multivariate, three-dimensional ECMWF optimum interpolation scheme in analysing the free modes of the global, multi-level ECMWF gridpoint model has been investigated. With the use of an idealised data coverage, several systematic deficiencies could be identified:

- the 'locality' of the scheme

- the tropical mass-wind coupling

- the poor specification of vertical correlations

While the last point is probably a particular feature of the ECMWF scheme (which is currently being investigated further), the other two points are of a more general nature. The 'locality' problem can perhaps be alleviated by a multi-pass system, where in each pass the response of the analysis operator is optimised for a particular spectral band. The tropical coupling problem can, however, not be overcome by such an approach. An obvious alternative would be a direct fit to some selected large scale modes. It is well known that best fit methods result in unrealistic fluctuations in data sparse areas. On the other hand, they would perhaps allow a better extraction of the large scale information from the irregularly, but not randomly spaced observation network. After all, the correction of a large scale first guess error must result in changes in data void areas.

While the experiments with the idealised data coverage helped to demonstrate some systematic problems, a possibly alarming result is the poor analysis of the largest scales when using a present-day observing network. Due to the

lack of data, the analysis error for the input mode itself can reach the 50% level. When horizontal and vertical aliasing is taken into account, typical RMS error are in the order of 75%. Some improvements might be obtained by refining the analysis scheme. A more direct effect should be obtained, though, by a more regular observation network.

Some points have not been covered in this paper. The question of the relevance of the initial state of the large scale flow for medium range weather forecasting has not yet been investigated systematically. Furthermore, it is not clear to what extent the results apply to a four-dimensional data assimilation system. If the first guess errors for the large scale flow are somehow smaller than the analysis errors, a longer assimilation might eventually converge to the correct answer. However, the presence of large scale systematic errors and of spin-up problems adds further complications.

Finally, it might be argued that single mode experiments are unfair for a statistical interpolation scheme which has been designed to yield reasonable results on a local scale, averaged over a number of realizations. For instance, the assumed first guess and observation errors are not uniform over the globe and necessarily lead to some aliasing. Also, in single mode experiments aliasing from smaller scales onto the larger scales cannot be included. Obviously, this type of error can have beneficial as well as detrimental effects. Even if it helps to reduce the large scale errors, it is the right result for the wrong reason; the spectra should then be interpreted with some reservation.

Clearly, the O/I formulation can be optimised for the analysis of the planetary scale. Even then some problems remain: how to extract the long wave information from the present network and how to treat the tropical mass-wind coupling.

REFERENCES

- Ahlquist, J.E. 1982 Normal-mode global Rossby wave: Theory and observations. *J.Atmos.Sci.*, 39, 193-202.
- Andersen, J.H. 1983 Experiments with increased vertical resolution in the ECMWF analysis system. ECMWF Workshop on "Current problems in data assimilation", 8-10 November 1982, 183-206.
- Hayashi, Y. and Goulder, D-G. 1978 The generation of equatorial transient planetary waves: Control experiments with a GFDL general circulation model. *J.Atmos.Sci.*, 35, 2068-2082.
- Holton, J.R. 1979 An introduction to dynamic meteorology. Academic Press, New York.
- Longuet-Higgins, M.S. 1968 The eigenfunctions of Laplace's tidal equations over a sphere. *Phil.Trans. of the Royal Society of London, Series A, No.1132*, 262, 511-607.
- Lorenc, A.C. 1981 A global three-dimensional multivariate statistical interpolation scheme. *Mon.Wea.Rev.*, 109, 701-721.
- Temperton, C. and Williamson, D.L. 1981 Normal mode initialisation for a multilevel gridpoint model. Part I: Linear aspects. *Mon.Wea.Rev.*, 109, 729-743.
- Yenne, D.E. and Stanford, J.L.S. 1982 An observational study of high-latitude stratospheric planetary waves in winter. *J.Atmos.Sci.*, 34, 1026-1034.
- Wergen, W. 1983 Forced motion in the tropics. ECMWF Workshop on "Current problems in data assimilation", 8-10 November 1982, 275-298.